Unsteady Aerodynamics Modeling for a Flexible Unmanned Air Vehicle

Aditya Kotikalpudi,* Harald Pfifer† and Gary J. Balas‡
Department of Aerospace Engineering & Mechanics
University of Minnesota, Minneapolis, MN, 55414, USA

An unsteady aerodynamics model of a flexible unmanned air vehicle is presented in this paper. The unsteady aerodynamics results from structural vibrations of the flexible airframe which affect the airflow around it. The doublet lattice method, which is a potential flow based panel method, is used for obtaining the basic unsteady aerodynamics model. It gives the pressure distribution on a lifting surface harmonically oscillating in steady flow. The basic concepts, underlying assumptions and approximations of the method are discussed. The extensive post processing which is done for the model obtained from the doublet lattice method is also described. The aerodynamic model is first transformed into suitable coordinates to account for structural vibrations effects. A rational function fitting is then carried out to obtain the final model which is suitable for time domain analysis. We use these methods to obtain an unsteady aerodynamics model of the Body Freedom Flutter vehicle, a flexible test bed aircraft. The results of this application are discussed. The final model is used for developing a nonlinear simulation for the flexible aircraft which is capable of simulating phenomena such as flutter and is important for integrated control law synthesis for the aircraft. The software for DLM as well as the post processing tools are made available as an open source research tool for aeroelastic systems research.

Nomenclature

$\bar{w}$	Component of flow velocity perpendicular to a surface, normalized by freestream airspeed
$\bar{p}$	Lifting pressure vector normalized by freestream dynamic pressure
ω	Oscillation frequency (rad/s)
k	Reduced frequency
AIC	Aerodynamics Influence Coefficients Matrix
V	Free stream airspeed (m/s)
η	Structural deflections in modal coordinates
T_{as}	Transformation matrix for obtaining aerodynamics in modal coordinates
Φ	Mode shapes
$Q(k)$	Generalized aerodynamics matrix (GAM), function of reduced frequency

I. Introduction

As modern aircraft designers focus on increased aerodynamic efficiency and low structural weight, the resulting designs often feature flexible airframes. That results in excitation of vibrational modes of the aircraft due to aerodynamic loads. This interaction between aerodynamics, structural dynamics and rigid body dynamics can cause structural fatigue and poor handling qualities of the aircraft. Also, in phenomena like body freedom flutter, where the first wing bending mode interacts with the rigid short period mode in an unstable manner, catastrophic failure and loss of aircraft can occur.[1,2] Hence, it is vital to understand and model the dynamics of flexible air vehicles for synthesizing controllers which are capable of both flight

*Graduate Student, AIAA Student Member
†Postdoctoral Associate
‡Professor, AIAA Associate Fellow

control as well as active flutter suppression in an integrated manner.

An important part of modeling the dynamics of a flexible aircraft is its unsteady aerodynamics. Unsteady aerodynamics modeling, which involves computation of the forces exerted on a body in a time dependent air flow, has been important for reliable flutter analysis. There are several methods available to study unsteady aerodynamics, ranging from advanced, high fidelity computational fluid dynamics (CFD) solvers,[3–5] to potential flow based aerodynamic strip theory, which utilizes 2-D infinite wing assumptions.[1,6] CFD methods provide models with very high number of states which are very computationally expensive to simulate and unsuitable for control design. On the other hand, strip theory based methods provide computationally inexpensive models, but they lack the desired fidelity we may require for aeroelastic analysis. Fortunately, potential flow based panel methods[7–9] developed in the 1960s and 1970s have successfully fulfilled the requirement of modeling techniques which are computationally inexpensive while modeling the lifting characteristics of finite wings with reasonable accuracy. For unsteady aerodynamics and flutter analysis, the most widely used panel method is known as the doublet lattice method (DLM).[10,11] The DLM provides low order models for unsteady aerodynamics, which lead to aeroelastic models suitable for control design. This is an attractive feature which is missing from the models obtained from CFD, which although rich in detail, have very large number of states which ultimately make control design infeasible. The only significant disadvantage of the DLM is its inability to model drag, since the method is based on potential flow theory.[12,13] However, since drag does not significantly affect flutter analysis, we choose DLM for modeling unsteady aerodynamics.

The unmanned aerial vehicle (UAV) research group at the University of Minnesota carries out extensive research in the field of aeroservoelastic control. The main application for the research so far has been the Body Freedom Flutter (BFF) aircraft constructed by the Air Force Research Laboratory (AFRL) and Lockheed Martin (LM) for research on flutter suppression control[2] (see section II). One of the ongoing research projects in the group is to develop a nonlinear simulation for the BFF aircraft which captures its aeroelastic behavior in the a frequency range of interest across its flight envelope.[14] The simulation requires an unsteady aerodynamic model which can be coupled with a structural dynamics model of the aircraft and enable aeroelastic analysis in the time domain. This paper describes the methods used to obtain the aerodynamic model for the BFF aircraft which is suitable for time domain analysis. The DLM is used to obtain an aerodynamic model as a function of oscillating frequency (see section III). The model is then made suitable for time domain analysis using Rogers approximation[15] (see section IV). The software for the method has been implemented in a modular manner, as described in section V. Finally, the resulting aerodynamic model is discussed in section VI.

The entire project follows the same open source philosophy which has been the hallmark of all the projects associated with the UAV group so far.[16] All the data regarding the aerodynamic design of the aircraft as well as the software for aerodynamic modeling can be downloaded from (`http://www.aem.umn.edu/~AeroServoElastic/`). It is hoped that the BFF aircraft will become an important resource and a benchmark for researchers in the fields of aeroelastic modeling and aeroservoelastic control.

II. Background: Body Freedom Flutter Aircraft

The BFF aircraft was jointly developed by the AFRL and LM to study the body freedom flutter, which involves the coupling of the first wing bending mode with the rigid short period mode. It creates a dynamic instability which if uncontrolled, leads to catastrophic failure and loss of aircraft. Multiple BFF aircraft were built, most of which were flown to the edge of their envelope and destroyed in flight. One BFF aircraft was donated to the UAV research group as mentioned, along with linear time invariant (LTI) models at airspeeds from 40 to 90 KEAS. Fig. 1 shows a computer aided design (CAD) implementation of the outer mold line of BFF aircraft, obtained via a laser scan conducted at the QC group, Minnesota.[17] This CAD model provides the geometry of the aircraft required for the aerodynamic grid. Fig. 1 shows the top view of the aircraft with the basic dimensions and control surface allocations for longitudinal (elevators) and lateral (ailerons) controls. The control surfaces dedicated to flutter suppression control are also indicated, which are used to delay the onset of body freedom flutter by damping the first symmetric wing bending mode as well as the rigid short period mode. The complete build details of the aircraft are accessible on the group website.[18]

A nonlinear model for the aircraft has been developed by following a subsystem based approach. Models for individual subsystems like aerodynamics, structural dynamics and rigid body dynamics have been

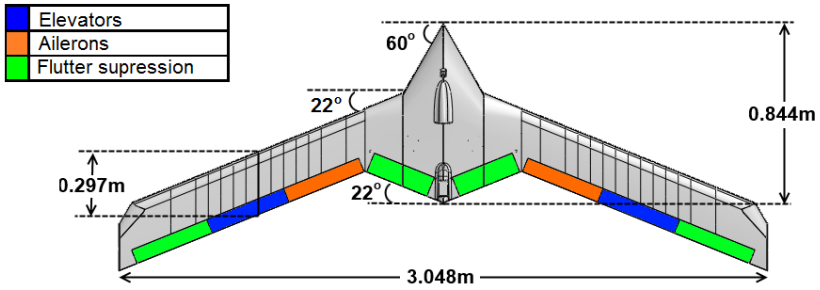

Figure 1. Top view of the BFF aircraft

developed separately and then combined to form the overall aeroelastic model. Other subsystems such as actuators and control laws can be easily added to get the overall aeroservoelastic model. Conceptually, the interconnection between various subsystems can be viewed as shown in Fig. 2.

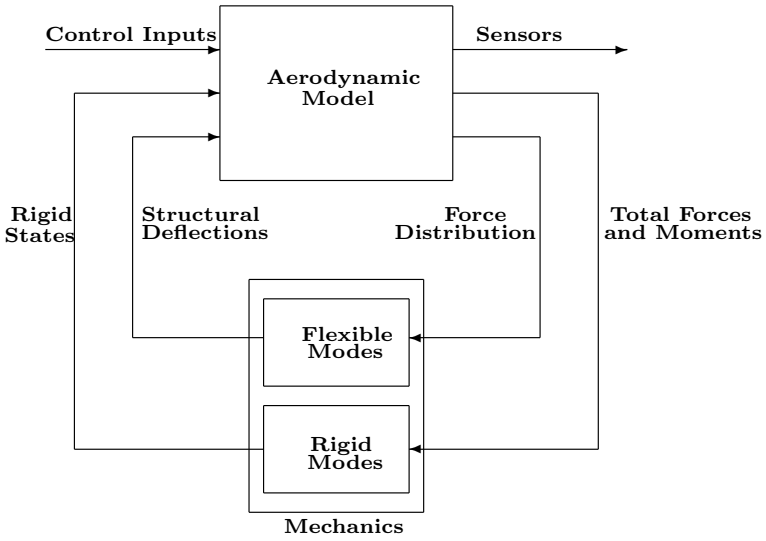

Figure 2. Subsystem interconnection

Since we develop the aerodynamic model and the mechanics model (consisting of the structural and rigid body models) separately using suitable modeling methodologies, this results in different choices of coordinates for different subsystems. These differences are resolved using suitable coordinate transformations so that the subsystems may be combined correctly to obtain the final aeroelastic model. We can see the motivation for such transformations as follows.

Fig. 3 shows an aerodynamic grid developed for the BFF aircraft, which typically consists of more than 1000 panels. The number of panels is governed by the complexity of the aircraft geometry, as well as certain requirements that need to be fulfilled for acceptable accuracy of the DLM, as discussed in section III. The DLM assumes each panel to move individually, which results in 1000's of degrees of freedom (DoF) in the aerodynamic model.

On the other hand, the structural model is obtained from a Finite Element (FE) approach, consisting of 14 nodes interconnected with linear beam elements[19,20] (Fig. 4). The node locations are decided on the basis of physical locations of components such as winglets, actuators, flight computer and other electronics. Since we opt to represent the structural model using simple beams, the number of elements required is quite

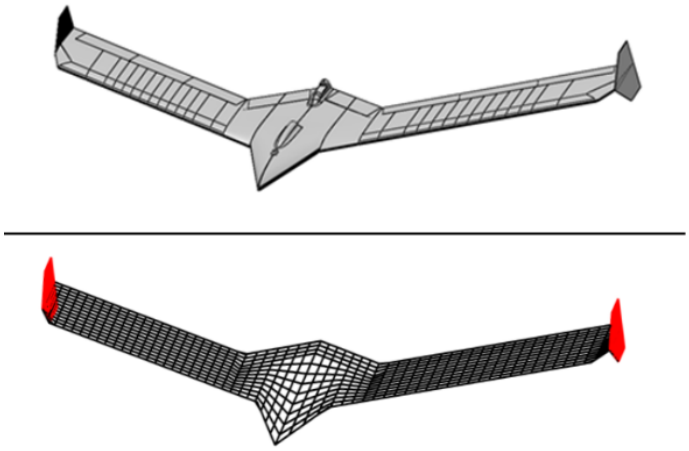

Figure 3. A CAD model of the BFF aircraft and the corresponding aerodynamic grid

small compared to the aerodynamic model. The center body of the aircraft is assumed rigid, which is why the elements representing the center body (nodes 1-5 and 10) are assumed to have very high stiffness.

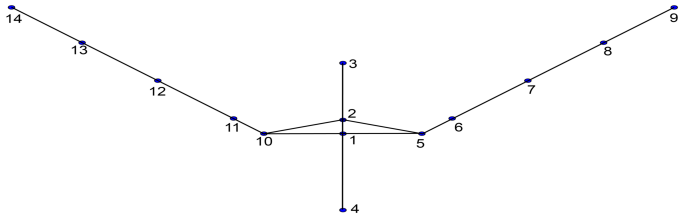

Figure 4. Finite element grid of the BFF aircraft

Due to the low number of nodes in the structural model, the DoF in the structural model is less than that of the aerodynamic model by of orders of magnitude. Hence, coordinate transformations are essential so that the effects of vibrations, expressed in the structural model coordinates, can be used as an input for the aerodynamic model, as shown in Fig. 2. This is discussed in detail in section IV. Finally, it should be mentioned that the UMN UAV group has built a rigid version of the BFF aircraft which is undergoing flight tests. The group is also building a series of flexible aircraft based on the same aerodynamic design, all of which will serve as open source test beds. Aeroelastic models for these aircraft will be also be available on the group website for the benefit of the research community.

III. The Doublet Lattice Method

This section describes the DLM method in a conceptual manner and its application to flexible lifting surfaces. The authors assume the reader to be familiar with potential flow theory and associated terminology, which is available for study in any basic textbook of aerodynamics.[12] Also, derivations and descriptions of the governing equations for the DLM are available in literature[10,21] and this paper will not discuss them.

The DLM is a potential flow based panel method developed in the 1960s by Albano & Rodden[10] to solve for unsteady aerodynamic flow across a lifting surface. It can also efficiently handle multiple surfaces and their interfering effects on one another. The method assumes the flow across a fixed surface to undergo harmonic oscillations. This is equivalent to the case where the surface undergoes harmonic oscillations in a steady flow since the DLM does not differentiate between these two cases. Pressure distribution across the surface is obtained as a solution for a given flow condition. Since the model obtained from DLM is linear, the solution is also a harmonic function with the same frequency. In other words, the DLM gives us a frequency

response for pressure distribution on an oscillating surface in steady flow, for a specific frequency.

The DLM is a panel method, which means that the surface is typically divided into small trapezoidal panels for computational purposes with a constant pressure distribution assumed on each panel, as shown in Fig. 5. The dashed lines represent a doublet line at the $^1/_4{}^{th}$ chord location of each panel. The points located at the $^3/_4{}^{th}$ chord location of each panel is the normalwash calculation point or the collocation point.[12,22] Normalwash is defined as flow normal to the surface at a given point, normalized by free stream flow speed and is a function of how the surface moves with respect to the free stream.

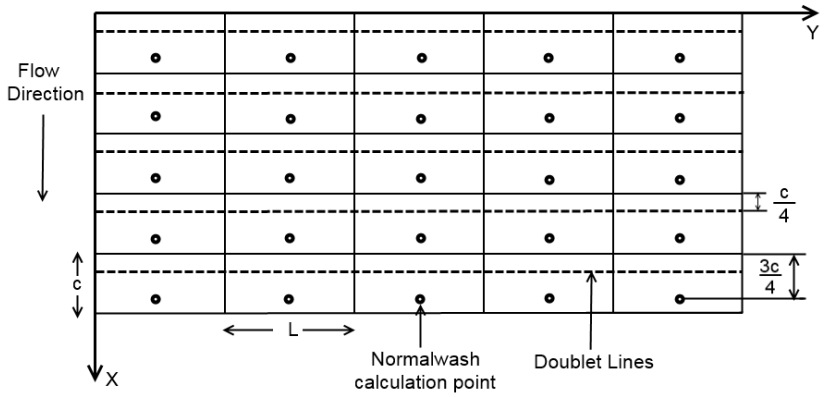

Figure 5. A typical discretization of the lifting surface S

When the lifting surface undergoes harmonic oscillations in pitch or heave in steady flow, normalwash is generated at each panel as a function of its location on the surface. For instance, if the surface shown in Fig. 5 oscillates in pitch about the leading edge (Y axis) with a given frequency and small amplitude, each panel experiences a normalwash proportional to the distance from Y axis. DLM uses this normalwash distribution to calculate the pressure differences across these panels. The final output of the DLM is given in Eq. 1 which relates the normalwash vector $\bar{w}$ containing the normalwashes at collocation points of all the panels, to the normalized pressure difference vector $\bar{p}$ about the panels.

$$\bar{p} = \big[AIC(\omega, V)\big]\bar{w} \tag{1}$$

Here, AIC is the aerodynamics influence coefficients matrix which is complex valued. It should be noted that both $\bar{w}$ and $\bar{p}$ are harmonic functions. The primary objective of the DLM is to compute the AIC matrix for a given aerodynamic grid, oscillating frequency and speed of the flow. The nature of the governing equations of the DLM allow us to combine the oscillating frequency (ω) and flow speed (V) into a single dimensionless parameter known as the reduced frequency k.

$$k = \frac{\omega \bar{c}}{2V} \tag{2}$$

where $\bar{c}$ is the reference chord length of the the aircraft under consideration. Thus, for a given panel grid, the AIC matrix is only a function of the reduced frequency.

From Eq. 1 we can see that essentially the oscillatory normalwashes of individual panels are required for calculating the pressure distribution. Therefore, although the method was developed assuming rigid motion of the lifting surface, it is applicable even if there is no such constraint on the motion of the panels. In other words, if an elastic deformation of the surface can be approximately discretized in terms of motion of the panels, the corresponding normalwash vector can be computed and Eq. 1 can be readily used to obtain the pressure distribution. This is the main philosophy behind using the DLM for aerodynamic modeling of flexible aircraft. This is further discussed in the next section.

Since the AIC matrix is constant for a given reduced frequency but complex valued, the pressure distribution is a harmonic function with the same frequency as the normalwashes but with a phase difference introduced by the AIC matrix. The resulting aerodynamic force distribution can be easily calculated as shown in Eq. 3.

$$F_{aero} = \bar{q} S_p [AIC(k)] \bar{w} \tag{3}$$

where $\bar{q}$ is the freestream dynamic pressure and S_p is the panel area matrix.

In order to get accurate models from the DLM, certain rules of thumb should be kept in mind, as listed below.

1. The aspect ratios of individual panels must not be greater than 3.[21,23]

2. There is a lower limit on the number of panels in the chordwise direction governed by the highest reduced frequency considered for analysis.[23] The thumb rule for calculating the number of panels is 8 to 12 per wavelength of the flow. The wavelength λ can be calculated from reduced frequency k and reference chord $\bar{c}$ using Eq. 4

$$\lambda = \frac{\pi \bar{c}}{k} \tag{4}$$

   Increasing the number of chordwise panels satisfies this thumb rule, but it also results in increase in panel aspect ratio for a given strip width, thus going against the first rule. Hence, the panels must be optimally constructed to satisfy these thumb rules while remaining as low in number as possible.

It should be emphasized that these are not hard constraints and should be considered as general rules of thumb. Convergence studies (see section V) should be conducted on a case to case basis for obtaining minimum number of panels required.

Finally, to ensure that the DLM converges to solutions obtained from a standard panel method like the Vortex Lattice Method (VLM)[12] for steady state, it is common practice to subtract out the steady part in the governing equations of DLM and replacing it with solutions from the VLM.[10,22] Hence, we have embedded a VLM module into the DLM software to ensure higher accuracy in the steady state solution.

IV. Generalized Aerodynamic Model

The DLM method described in section III provides the aerodynamic force distribution for a given normalwash distribution on the aerodynamic grid (Fig. 5) at a particular oscillating frequency. However, the aerodynamic model should be able to effectively interact with the corresponding structural model built for the design to produce coupled aeroelastic phenomena such as flutter. For that, there has to be a way to generate normalwash distribution for a given elastic deformation which is provided by the structural grid. Also, the effect of the aerodynamic forces computed in Eq. 3 on the structural model has to be computed. Finally, we need a continuous frequency domain model to carry out aeroelastic analysis as desired. In this section, we address these issues with the help of an example problem. Consider a surface with just four panels, as shown in Fig. 6.

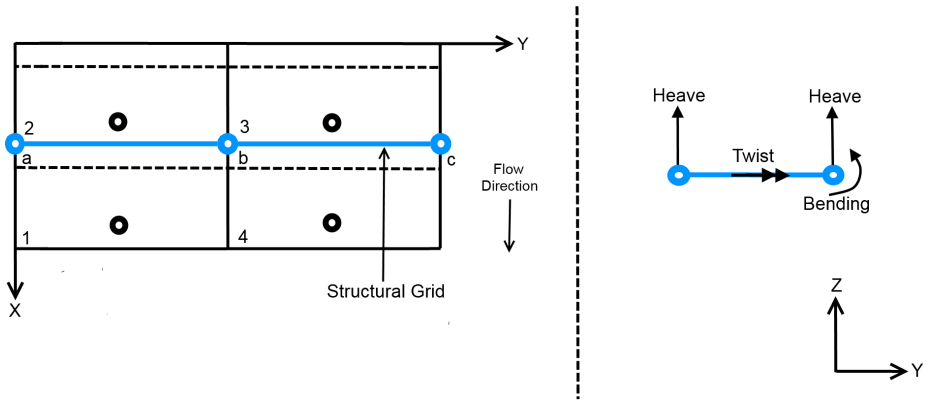

Figure 6. The 2×2 grid example in top view, with a superimposed finite element structural model. Also shown are beam DoF

Fig. 6 shows a finite element (FE) grid created for the lifting surface, superimposed on the aerodynamic grid used in the unsteady aerodynamics model. The FE grid is similar to the one described for the BFF aircraft in section II. As seen in the figure, beam elements interconnecting the three nodes are allowed to bend about the x-axis, twist about the y-axis and heave in the direction of z-axis, giving a total of 3 DoF to each of the nodes a, b and c. For the aerodynamic panels, 2 DoF each are considered which are pitch about centerline parallel to Y axis and heaving motion, which result in change in the normalwash experienced by them. We need a way to project the DoF of the structural grid on to the aerodynamic panels so that the normalwash vector may be calculated for a given elastic deformation. This is done by computing suitable coordinate transformation matrices, which is discussed ahead.

A. Generalized Aerodynamics Matrices

The first step is to express structural deformations obtained from structural models in terms of the aerodynamic panels. The structural model can essentially be expressed in modal coordinates via modal decomposition the FE model.[24,25] The structural model can be written as

$$M\ddot{\eta} + C\dot{\eta} + K\eta = F_{modal} \tag{5}$$

where M, C and K are the modal mass, damping and stiffness matrices respectively, while F_{modal} is the external excitation in modal coordinates. Thus, an elastic deformation of the i^{th} node in physical space given by δ_i is expressed in terms of modal coordinates using the mode shapes Φ.

$$\delta_i = \sum_{j}^{n} \Phi_{ij}\eta_j \tag{6}$$

Next, to project this set of nodal displacements on to the aerodynamic model, we construct a spline grid based on the existing structural grid as shown in Fig. 7.

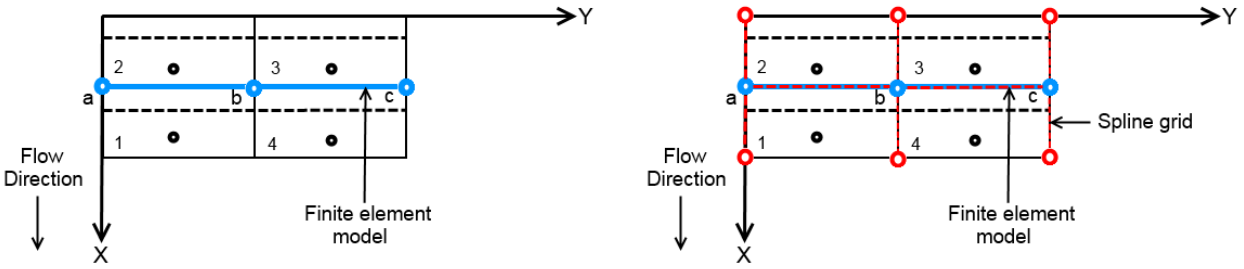

(a) Structural grid

(b) Spline grid

Figure 7. Spline grid construction

Each of the red connections of the spline grid is assumed to be stiff. The purpose of the spline grid is to transform all the DoF of a node on the structural grid into pure heaving motion of the spline grid nodes attached to it. For example, a twisting motion of the beam element attached to node c can be represented as asymmetric heaving motion of the spline nodes attached to node. Of course, this is only valid for small deflections, but then so is the linear structural model. We assume this transformation to be represented by the matrix T_{spline}.

The spline grid is assumed to be attached to an infinite plate and move in a rigid manner according to the structural grid as described. Radial basis functions[26,27] are then used to calculate displacements at locations on the infinite plate which specify the aerodynamics panels, by interpolating between displacements of the spline grid nodes. The motion of the aerodynamic panels is described in terms of their mid-points. For example, the heave of a panel is calculated in terms of the heave of its mid point (i.e. mid point of its center chord) while pitching of the panel is calculated as the rotation about its mid point. Thus, the relative heaving of the spline nodes is interpolated to obtain pitch and heave of the aerodynamic panels. This interpolation operation can be expressed in the form of a matrix $T_{inpterp}$. We can then evaluate T_{as} as

$$T_{as} = \big[T_{interp}\big]\big[T_{spline}\big] \tag{7}$$

Thus, we obtain T_{as} matrix which projects the structural grid deformation on to the aerodynamic panels in form of their pitch and heave in a linear manner, which is valid for small deformations.

Next step is to calculate the normalwash on the panels due to a given pitch and heave motion. This is done by constructing the so called differentiation matrices D_1 and D_2 as shown in [22]. For the example above, let the degrees of freedom for panel 1 be expressed as $\left[\begin{smallmatrix}\theta_1\\ h_1\end{smallmatrix}\right]$, where θ_1 and h_1 are the pitch and heave displacements respectively. It can be deduced that a heave displacement does not have any contribution to normalwash at the panel collocation point where the normalwash has to be calculated, while a pitch displacement results in an equal amount of normalwash for small angles. Similarly, both heave velocity ($\dot{h}_1$) and pitch rate ($\dot{\theta}_1$) induce normalwash at the collocation point given by $\big(-\frac{\dot{h}_1}{V}\big)$ and $\big(\frac{\dot{\theta} c_1}{4V}\big)$, respectively. Here, c_1 is the average chord of panel 1, which means that the moment arm between the mid-point and collocation point is $\frac{c_1}{4}$. Thus, the D_1 and D_2 matrices and the total normalwash expression can be written as

$$D_1 = [1 \quad 0] \tag{8a}$$

$$D_2 = \frac{2}{\bar{c}}\left[\frac{c_1}{4} \quad -1\right] \tag{8b}$$

$$\bar{w_1} = D_1[\theta_1 \quad h_1]^T + D_2[\dot{\theta}_1 \quad \dot{h}_1]^T \frac{\bar{c}}{2V} \tag{8c}$$

In D_2, we normalize the matrix with the reference chord $\bar{c}$ which appears in the expression for reduced frequency. This is done so that the factor $\frac{\bar{c}}{2V}$ can be isolated as seen in Eq. 8c. Since θ_1 and h_1 are harmonic functions of frequency ω as seen in Eq. 9a,b we can rewrite $\dot{\theta}_1$ and $\dot{h}_1$ as shown.

$$\theta_1 = \theta_0 e^{i\omega t} \tag{9a}$$

$$h_1 = h_0 e^{i\omega t} \tag{9b}$$

$$\dot{\theta}_1 = i\omega\theta_1 \tag{9c}$$

$$\dot{h}_1 = i\omega h_1 \tag{9d}$$

Equation 8c can now be rewritten in terms of these Fourier transforms as

$$\bar{w_1} = (D_1 + ikD_2)[\theta_1 \quad h_1]^T \tag{10}$$

Here we have used Eq. 2 to express the normalwash of panel 1 as a function of reduced frequency k. We can similarly compute D_1 and D_2 matrices for all the other panels and combine them in a block diagonal manner to obtain the complete normalwash vector for all the panels. From here on, D_1 and D_2 matrices would refer to the overall block diagonal matrices developed for all the panels. Finally, by combining Eqs. 10, 6 and transformation matrix T_{as}, we can write Eq. 11.

$$\bar{w} = (D_1 + ikD_2)T_{as}\Phi\eta \tag{11}$$

Thus, we have the equation for calculating the normalwash vector for DLM from the modal displacement vector as required. The aerodynamic force distribution can now be written as shown in Eq. 12

$$F_{aero} = \bar{q}S\big[AIC(k)\big](D_1 + ikD_2)T_{as}\Phi\eta \tag{12}$$

This force distribution acts as the external excitation for the structural model expressed in Eq. 5. However, F_{aero} obtained from Eq. 12 is on the aerodynamic panels. Therefore, the final step is to obtain the force distribution in modal coordinates using the same transformation matrices T_{as} and Φ.

$$F_{modal} = \Phi^T T_{as}^T F_{aero} \tag{13}$$

Combining Eqs. 12 and 13 and leaving out the dynamic pressure term $\bar{q}$ and the modal coordinate term η, we obtain the equation for the so called generalized aerodynamics matrix (GAM).

$$Q(k) = \Phi^T T_{as}^T S[AIC(k)](D_1 + ikD_2)T_{as}\Phi \tag{14}$$

which maps modal deformations to the aerodynamic force distribution which is also in modal coordinates as shown in 15.

$$F_{modal} = \bar{q}\big[Q(k)\big]\eta \tag{15}$$

In other words, the GAM is the unsteady aerodynamic model expressed in the structural modal coordinates. It should be noted that although the structural grid, spline grid and the aerodynamic grid in the example have a similar number of DoF, the method described in this section is applicable even when the grids have DoF orders of magnitude apart as we know is the case with the BFF aircraft.

B. Rational Function Approximation

The GAM matrices are obtained for discrete reduced frequencies. However, a continuous model is required for time domain aeroelastic simulations. Several methods have been developed to obtain such models[15,28,29] from the frequency response data. Roger's method[15] is one of the most prevalent methods used for this purpose which basically involves a function fitting for the GAM matrices at various reduced frequency.

Following Roger's method, GAM matrices can computed for different reduced frequencies and then fitted to a predefined rational function using a least squares technique. A rational function approximation (RFA) is done for the GAM matrices so that the aerodynamic model is of the form

$$Q(k) = Q_0 + Q_1 ik - Q_2 k^2 + \sum_{l=1}^{n} Q_{l+2}\frac{ik}{ik + b_l} \tag{16}$$

Here, Q_0, Q_1 and Q_2 represent the quasi-steady, velocity and acceleration terms of the aerodynamic model respectively. The Q_{l+2} terms take into account the lag behavior of unsteady flow. In order to keep the fitting linear so as to be able to use a least squares approach for RFA, the poles b_l for the aerodynamic lag states are to be chosen by the user iteratively until good fits are obtained. It can be seen that since k is a function of airspeed, the aerodynamic model is actually linear parameter varying (LPV)[30] with respect to velocity. Although we could have chosen to carry out RFA of the AIC matrix itself and then carry out the coordinate transformation later, it should be remembered that the AIC matrix is a square matrix of order equal to the number of aerodynamic panels. It is much more convenient to do the RFA for the GAM matrices which have the same low order as the structural model. At the end of the post processing described in this section, we finally have an unsteady aerodynamic model suitable for coupling with the structural model and further time domain analysis.

V. Open Source Software Tools

MATLAB based software tools have been developed to carry out the unsteady aerodynamics modeling procedure discussed in the preceding sections. Although currently the main application is the BFF aircraft, the tools have been developed keeping general applications in mind. All the functionalities are completely modular, enabling their use individually or together as required. The important functionalities of the software are

DLM code: Core implementation of the DLM method described in literature. It requires as inputs the aerodynamic grid, reduced frequency and Mach number. It computes the AIC matrix as the output.

VLM code: Implementation of the VLM method. Although the function is used within the DLM code, it is modular so that it can be used independently for steady aerodynamic modeling.

GAM generation: Contains the codes for constructing spline grid from a given structural grid, compute the transformation matrix T_{as} and GAM. Also, contains a code for implementing a least squares based RFA.

BFF model example: Contains the setup file, griding functions for aerodynamic panel generation and aircraft parameters for the BFF aircraft.

A basic validation of the software is presented here by comparing data generated for a test case to the published data. A test case taken from a paper by William Rodden et al[23] which considers the simple grid layout of 5x5 panels shown in Fig. 5. The aspect ratio of each panel is 5 while the flow parameters Mach number and reduced frequency are 0.8 and 2 respectively. The doublet strength distribution is computed for the doublet line of the middle panel of the grid. The results from the paper[23] are superimposed on the results obtained from the software in Fig. 8, which verify the DLM implementation.

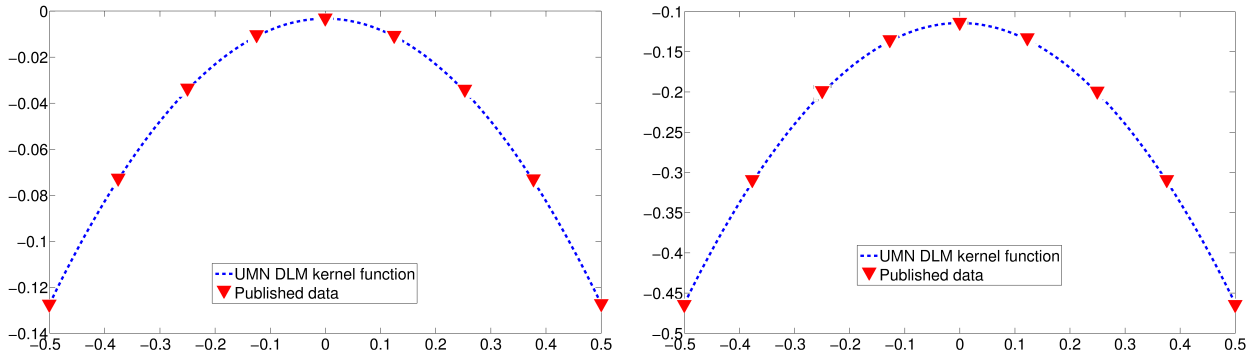

(a) real part (b) Imaginary part

Figure 8. Kernel function distribution on a panel of AR= 5 at k = 2 and Mach no. = 0.8

The VLM code used for steady solution of the aerodynamic model is also validated against an open source, widely used VLM software called XFLR-5[31] via comparison of the conventional stability derivatives obtained from both.

The software is fully documented and is available for free download at the group website `http://www.aem.umn.edu/~AeroServoElastic/`. It is intended that the software tools developed by the group prove useful as open source research tools for the research community.

VI. Results for BFF aircraft

A. Convergence Tests

Fig. 3 shows a typical aerodynamic grid generated by the software for the BFF aircraft. To find the minimum number of panels for a reasonably accurate aerodynamic model, convergence tests were carried out by increasing panel density and checking for convergence in the solutions. It has been recommended that such tests should be carried out each time a new lifting surface is analyzed using the DLM.[23] These convergence tests provide a perspective on the rules of thumb mentioned in section III regarding panel aspect ratios and chordwise number of panels.

The tests are carried out by first evaluating the GAM matrices for a fixed reduced frequency value $k = 3$, keeping the chordwise divisions fixed and gradually increasing the spanwise divisions. This reduces the aspect ratio of the individual panels, and the entries of the GAM matrix are expected to converge. The number of chordwise panels is fixed to 12 panels per wavelength (Eq. 4). For $k = 3$, that corresponds to approximately 26 panels per strip for the BFF aircraft. Here, a *strip* is defined as the space between 2 spanwise division lines. Therefore, N spanwise division lines (including outermost lines) would result in $N - 1$ strips on the aircraft. The convergence of the real part of an element of the GAM matrix which represents lifting force due to first symmetric bending mode is seen in Fig. 9

It can be seen that the element considered in Fig. 9 has a value of -6.36 for spanwise divisions as 75, which has a convergence error of less than 1%. This trend is observed across all entries in the GAM matrix. The next step is to find the minimum number of chordwise panels required keeping the number of spanwise divisions constant at 75. The chordwise divisions are now gradually increased from 4 to 26. The results are shown in Fig. 10 for the same element shown in Fig. 10.

From Fig. 10 it can be concluded that for chordwise divisions of over 12 panels, the error is around 5% of the value -6.36 obtained from Fig. 9, which was achieved at 26 panels. In other words, we can get away

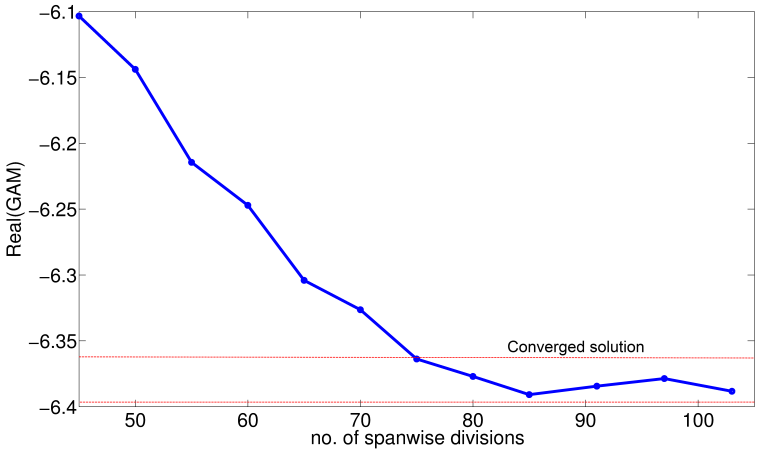

Figure 9. Convergence of the GAM matrix for k = 3, variation in spanwise divisions

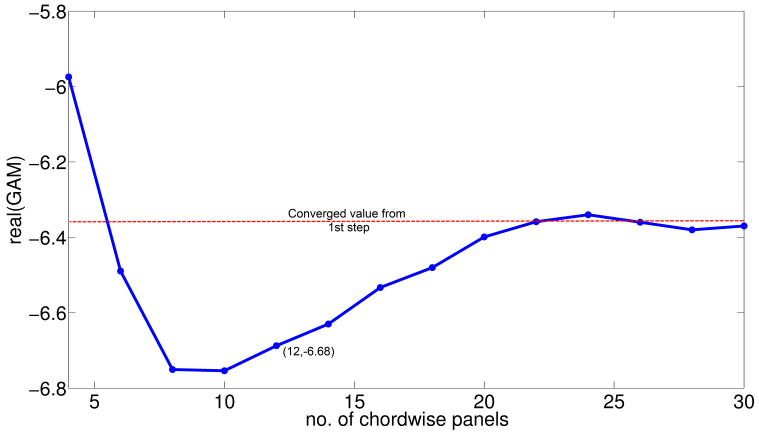

Figure 10. GAM matrix for k = 3, variation in chordwise divisions

with less than 6% error by reducing the number of chordwise panels from 26 to 12. For increased accuracy, higher number of panels can always be chosen, which would in turn result in higher computational effort. From this analysis for the BFF aircraft, the minimum number of spanwise is taken to be 75, which would result in 74 strips on the wing. The number of chordwise panels per strip is fixed at 12. A similar analysis for panels on winglets gives the number of panels per strip to be 10 and number of spanwise divisions to be 15. The total number of panels on the entire aircraft works out to be 1168. The maximum aspect ratio comes out to be 1.94, which is below the maximum threshold of 3 as discussed in section III.

B. Generalized Aerodynamic Model for the BFF aircraft

The final, transfer function based aerodynamic model is obtained by carrying out rational function fitting of the GAM matrices for the BFF aircraft, following the procedure laid out in section IV. A spline grid is constructed using the structural grid (Fig. 4) as the base, as seen in Fig. 11. This allows us to compute the transformation matrix T_{as}.

Here, it should be noted that the structural grid has 14 nodes with 3 DoF each, similar to the nodes in Fig. 6. This gives the total number of DoF for the structural grid to be 42. On the other hand, the aerodynamic grid has 1168 panels and each of them have 2 DoF. Therefore, the transformation matrix T_{as} interpolates between the 42 DoF of the structural grid and 2336 DoF of the aerodynamic panels. Also, it can be seen that carrying out the RFA fitting for the GAM matrices is computationally less expensive compared to doing it for the actual AIC matrices, since the GAM matrices are of the same order as the low order

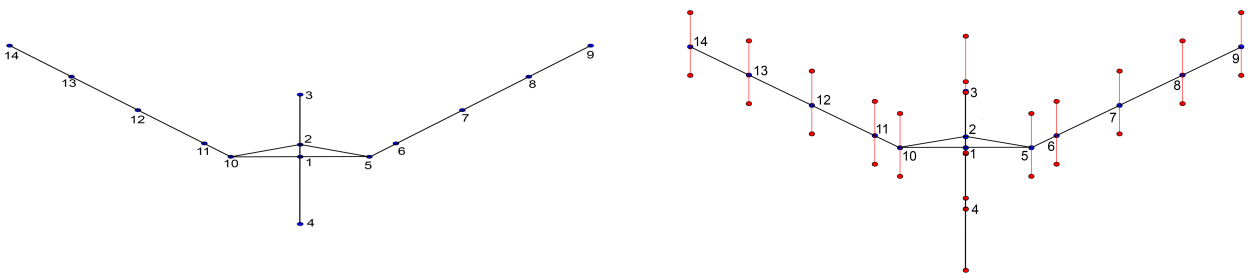

(a) Structural grid (b) Spline grid

Figure 11. Spline grid construction of the BFF aircraft

structural model. Once the T_{as} matrix is computed, the GAM matrices are computed using Eq. 14.

For carrying out the RFA, we calculate the AIC matrices at 8 different reduced frequencies ranging from 0 to 3. This range is chosen keeping in mind that according to Lockheed Martin flight test results,[2] the body freedom flutter occurs at a reduced frequency of about 0.23. The chosen range therefore ensures that all the necessary dynamics are captured by the model. The GAM matrices are then calculated for these 8 frequencies and the RFA is carried out to give the final aerodynamics model in a MIMO transfer function form as seen in Eq. 16. As mentioned earlier, the Roger's method is used for the RFA, which requires the poles for lag states to be specified apriori. A second order lag is chosen for the BFF aircraft and the poles are fixed to 0.11 and 0.22. It should be noted that the fitting is done for the dimensionless reduced frequency domain and the poles in actual frequency domain will vary with airspeed.

Fig. 12 shows the frequency responses of the aerodynamics transfer functions from the first symmetric bending mode and from elevator to lift force at 25 m/s airspeed. They also show the raw GAM matrix data from which these transfer functions have been fitted using the RFA function of the software.

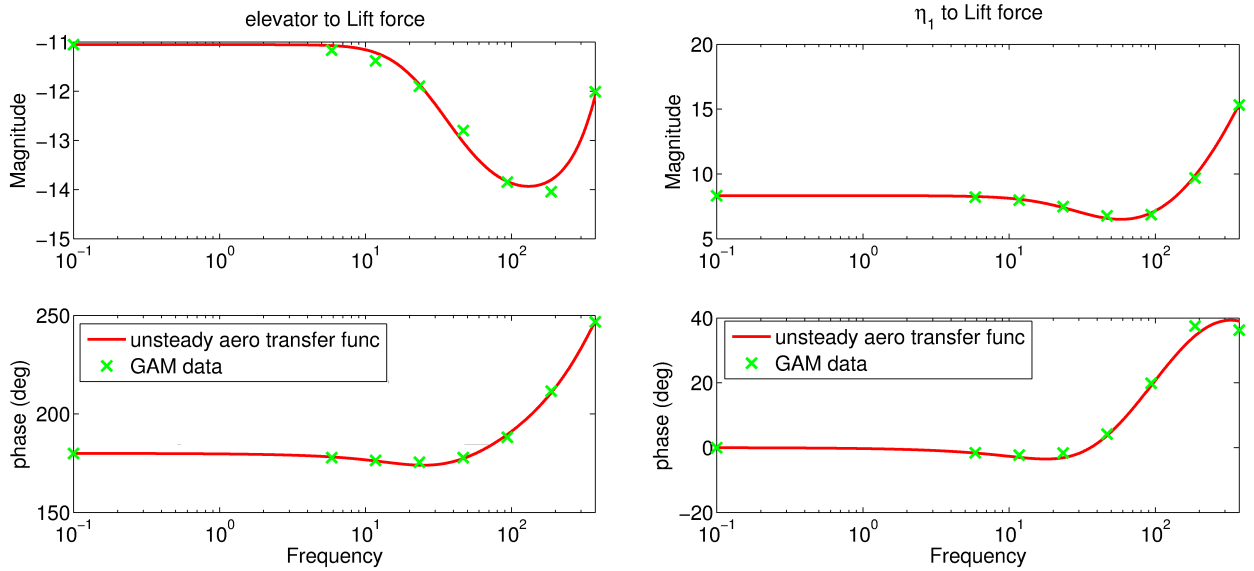

(a) Elevator to Lift (b) First symmetric bending mode to lift

Figure 12. Unsteady aerodynamics transfer functions for the BFF aircraft

The plots in Fig. 12 show lag behavior starting from approximately 10 rad/s, which at higher frequencies is dominated by the acceleration term in Eq. 16. This agrees with the fact that at the given velocity of 25 m/s, the poles of the second order lag are 13.5 and 27 rad/s. Fig. 13 shows the same transfer functions across a range of velocities between 20 and 50 m/s.

It can be seen that the onset of unsteady effects is delayed with increase in velocity. That agrees with

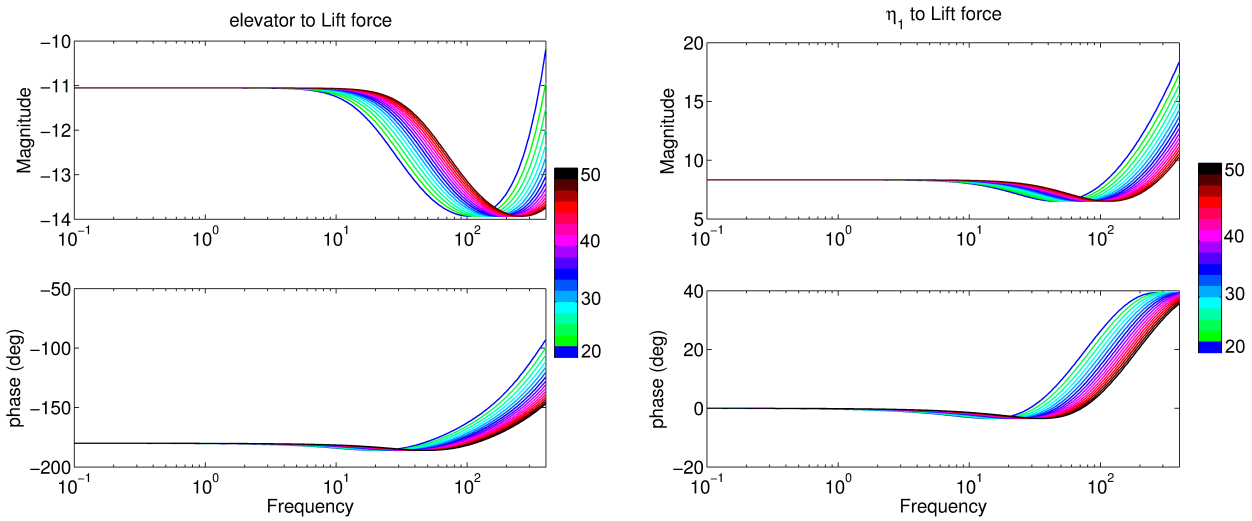

(a) Elevator to Lift

(b) First symmetric bending mode to lift

Figure 13. Aerodynamics transfer functions for the BFF aircraft from 20 to 50 m/s

the fact that the aerodynamic lag poles in the actual frequency domain increase in magnitude with increase in velocity. Also, the linear parameter varying nature of the aerodynamics becomes apparent beyond 10 rad/s, since the aerodynamics can be seen to visibly change with airspeed. This model therefore, is the first step towards LPV analysis of aeroservoelastic systems for model reduction, control design and various other applications.

Conclusion

A doublet lattice based unsteady aerodynamic model for the BFF aircraft has been developed which can be easily coupled with the structural model of the aircraft to construct an aeroelastic simulation in time domain. The software developed for the analysis is flexible for general applications that the group and the research community in general may work with. The aerodynamic models obtained are LPV in nature, with airspeed as the varying parameter. This will facilitate LPV model reduction and development of LPV controllers for integrated flight control and flutter suppression, which are the future objectives of the group. The aircraft has the potential of becoming a unique benchmark for unsteady aerodynamics modeling since along with the final unsteady model and detailed description of the BFF aircraft design, the tools used for the analysis have also been made available, so that the results obtained in this paper can be easily reproducible by the readers. This gives an opportunity to the research community to compare their analysis techniques against the DLM either by using the software for their research objective or by using their modeling technique on the BFF aircraft and compare the results against the model provided.

Acknowledgments

This work is supported by the NASA Phase II SBIR contract No. A2.04-8418 entitled Reduced Order Aeroservoelastic Models with Rigid Body Modes as a subcontract from Systems Technology Inc. Dr. Peter Thompson is the principal investigator and Dr. Martin Brenner is the NASA technical monitor. The authors also gratefully acknowledge Systems Technology Inc. for providing an initial code of the DLM method.

References

[1]Waszak, M. R. and Schmidt, D. K., "Flight dynamics of aeroelastic vehicles," *Journal of Aircraft*, Vol. 25, No. 6, 1988, pp. 563–571.

[2]Burnett, E., Atkinson, C., Beranek, J., Sibbitt, B., Holm-Hansen, B., and Nicolai, L., "NDoF Simulation model for flight control development with flight test correlation," *AIAA Modeling and Simulation Technologies Conference*, Vol. 3, 2010, pp.

7780–7794.

[3]Obayashi, S. and Guruswamy, G. P., "Convergence acceleration of a Navier-Stokes solver for efficient static aeroelastic computations," *AIAA journal*, Vol. 33, No. 6, 1995, pp. 1134–1141.

[4]Petterson, K., "CFD analysis of the low-speed aerodynamic characteristics of a UCAV," *AIAA Paper*, Vol. 1259, 2006, pp. 2006.

[5]Farhat, C., Lesoinne, M., and Le Tallec, P., "Load and motion transfer algorithms for fluid/structure interaction problems with non-matching discrete interfaces: Momentum and energy conservation, optimal discretization and application to aeroelasticity," *Computer methods in applied mechanics and engineering*, Vol. 157, No. 1, 1998, pp. 95–114.

[6]Rodden, W. P. and Stahl, B., "A strip method for prediction of damping in subsonic wind tunnel andflight flutter tests." *Journal of Aircraft*, Vol. 6, No. 1, 1969, pp. 9–17.

[7]Belotserkovskii, S. M., "Study of the unsteady aerodynamics of lifting surfaces using the computer," *Annual Review of Fluid Mechanics*, Vol. 9, No. 1, 1977, pp. 469–494.

[8]Hough, G. R., "Remarks on vortex lattice methods." *Journal of Aircraft*, Vol. 10, No. 5, 1973, pp. 314–317.

[9]Lan, C. E., "A quasi-vortex lattice method in thin wing theory," *Journal of Aircraft*, Vol. 11, No. 9, 1974, pp. 518–527.

[10]Albano, E. and Rodden, W. P., "A doublet-lattice method for calculating lift distributions on oscillating surfaces in subsonic flows." *AIAA journal*, Vol. 7, No. 2, 1969, pp. 279–285.

[11]Rodden, W. P., Taylor, P. F., and McIntosh, S. C., "Further refinement of the subsonic doublet-lattice method," *Journal of Aircraft*, Vol. 35, No. 5, 1998, pp. 720–727.

[12]Katz, J. and Plotkin, A., *Low speed aerodynamics: From wing theory to panel methods*, New York: Mc–Graw-H ill Book Co, 1991.

[13]Houghton, E. L. and Carpenter, P. W., *Aerodynamics for engineering students*, Butterworth-Heinemann, 2003.

[14]Kotikalpudi, A., Moreno, C., Taylor, B., Pfifer, H., and Balas, G., "Low cost development of a nonlinear simulation for a flexible uninhabited air vehicle," *American Control Conference (ACC), 2014*, IEEE, 2014, pp. 2029–2034.

[15]Roger, K. L., "Airplane math modeling methods for active control design," *Advisory Group for Aerospace Research and Development CP-228*, 1977, pp. 4–1.

[16]Dorobantu, A., Johnson, W., Lie, F. A., Taylor, B., Murch, A., Paw, Y. C., Gebre-Egziabher, D., and Balas, G., "An airborne experimental test platform: From theory to flight," *American Control Conference*, 2013, pp. 659–673.

[17]"QC group, Minnetonka, MN," *https://www.qcgroup.com*.

[18]"UAV research group, University of Minnesota," *https://www.uav.aem.umn.com*.

[19]Rodden, W. P., "A method for deriving structural influence coefficients from ground vibration tests." *AIAA Journal*, Vol. 5, No. 5, 1967, pp. 991–1000.

[20]Gupta, A., Moreno, C., , Pfifer, Harald Taylor, B., and Balas, G., "Updating a finite element based structural model of a smalll flexible aircraft," *AIAA Scitech Conference, 2015*.

[21]Blair, M., "A compilation of the mathematics leading to the doublet lattice method," Tech. rep., DTIC Document, 1992.

[22]Kier, T. and Looye, G., "Unifying manoeuvre and gust loads analysis models," *International Forum on Aeroelasticity & Structural Dynamics*, 2009.

[23]Rodden, W., Taylor, P., and McIntosh, S., "Improvements to the Doublet-Lattice Method in MCS/NASTRAN," *MacNeal-Schwendler Corp., Technical Rept., Los Angeles, Sept*, 1999.

[24]Fowles, G. R. and Cassiday, G. L., *Analytical mechanics*, Saunders College, 1999.

[25]Zienkiewicz, O. C. and Morice, P., *The finite element method in engineering science*, McGraw-hill, 1971.

[26]Buhmann, M. D., *Radial basis functions: theory and implementations*, Vol. 12, Cambridge University Press, 2003.

[27]Rodden, W. P. and Johnson, E. H., *MSC/NASTRAN Aeroelastic Analysis: User's Guide, Version 68*, MacNeal-Schwendler Corporation, 1994.

[28]Vepa, R., "Finite state modeling of aeroelastic systems," 1977.

[29]Karpel, M., *Design for active and passive flutter suppression and gust alleviation*, Vol. 3482, National Aeronautics and Space Administration, Scientific and Technical Information Branch, 1981.

[30]Tóth, R., *Modeling and identification of linear parameter-varying systems*, Vol. 214, Springer, 2010.

[31]"XFLR-5, open source VLM software," *http://www.xflr5.com*.